

Stabilized DSG Elements – A New Paradigm in Finite Element Technology

Authors:

Manfred Bischoff, Frank Koschnick, Kai-Uwe Bletzinger
Lehrstuhl für Statik
Technische Universität München

Correspondence:

Manfred Bischoff
Lehrstuhl für Statik
TU München
D-80290 München
Germany

Tel: +49-(0)89-28922435
Fax: +49-(0)89-28922421
e-mail: bischoff@bv.tum.de

Keywords:

finite element technology, locking, DSG method

ABSTRACT

The Discrete Shear Gap Method, initially proposed for the elimination of transverse shear locking in plate and shell finite elements is extended to a more general concept, applicable to other locking problems, typically causing severe trouble in structural analysis, especially in the case of thin-walled structures. The outstanding feature of the proposed formulation is the fact that one unique method is used to avoid various different kinds of locking phenomena. It is applicable to beam plate and shell elements, but also to two-dimensional and three-dimensional solid elements. The fact that approximation quality is often subject to strong sensitivity to mesh distortion can be alleviated with the help of stabilization methods.

INTRODUCTION

After more than thirty years of intensive research in finite element technology there is still a number of open issues. Today, mostly reduced integration along with hour-glass control or alternative finite element formulations (e.g. assumed strain elements or mixed hybrid methods) are applied. In both cases there are still problems, like "low energy modes", distortion sensitivity and the fact that triangles and tetrahedrons usually perform unsatisfactorily.

As a possibility to overcome the problem of transverse shear locking in plates and shells Bletzinger et al. [4] proposed the Discrete Shear Gap (DSG) method. The method has certain similarities to existing concepts, like the Assumed Natural Strain (ANS) method (also called MITC method), but it has some unique features: First, it is directly applicable to both triangles and quads, without any further considerations, like a particular choice of sampling points or the introduction of additional nodes or degrees of freedom. Second, it applies directly to elements of arbitrary polynomial order.

Of course, interest focuses on lower order elements, in particular three-node and four-node elements. The four-node DSG element turns out to be exactly equivalent to the corresponding ANS-element (the MITC-4 or "Bathe-Dvorkin element" [7]). The linear triangle, however, does not seem to have any correspondent in the literature. Due to the fact that for the latter one-point integration suffices, while its accuracy comes close to the four-node element, this seems to be a particular attractive choice for large scale computations of shells.

In the present paper, the DSG method is extended to a more general concept which is applicable to all kinds of structural finite elements. It turns out that the principal idea, initially tailored to tackle only transverse shear locking, is suited to handle all kinds of geometric locking effects, i.e. all locking effects which depend on certain geometric parameters like the shell thickness or the element aspect ratio.

Model Problem: Linear Timoshenko Beam Element

In order to explain the basic idea of the concept we consider a linear Timoshenko beam finite element. The kinematic equation for the transverse shear strain reads

$$\gamma = w' + \beta, \quad w' = \frac{dw}{dx} \quad (1)$$

with

$$\begin{Bmatrix} w \\ \beta \end{Bmatrix} = \frac{1}{2}(1-\xi) \begin{Bmatrix} w^1 \\ \beta^1 \end{Bmatrix} + \frac{1}{2}(1+\xi) \begin{Bmatrix} w^2 \\ \beta^2 \end{Bmatrix}, \quad -1 \leq \xi \leq 1. \quad (2)$$

It is well-known that the reason for shear locking is the linear interpolation of the displacement field w , such that w' is constant within the element. Thus, a pure bending deformation (with no shear deformation, i.e. $\gamma = 0$), where the rotation β is linear, cannot be represented with γ being identically zero within the element. Most of the popular concepts, like reduced integration or collocation of shear strains (assumed strain method), relax the resulting over-constraint by concentrating the condition $\gamma = 0$ to one single point. The DSG method works quite similar.

The first step is to split the transverse deflection w into a part w_γ , depending on the transverse shear strains, and a part w_β which belongs to bending. This split is uniquely obtained by integration of the kinematic equation

$$w_\gamma(\hat{x}) = w(\hat{x}) - w_\beta(\hat{x}) = \int_0^{\hat{x}} w'(x) dx - \int_0^{\hat{x}} \beta(x) dx, \quad 0 \leq \hat{x} \leq \ell. \quad (3)$$

Note that w_β is quadratic in a linear element, which is exactly the order needed for a constant bending moment according to the underlying differential equation. The function $w_\gamma(\hat{x})$ can also be denoted as a shear 'gap' because it represents the difference between the total deformation and the deformation due to bending – thus shear deformation.

Clearly, for pure bending w_β should be identically zero, which is not true in the element *domain* when linear shape functions are used (the reason for locking). But it does hold at the *nodes*. The obvious idea is thus to compute *discrete* shear gaps at the nodes

$$w_\gamma^1 = w_\gamma(0) = \int_0^0 w'(x) dx - \int_0^0 \beta(x) dx = 0, \quad (4)$$

$$w_\gamma^2 = w_\gamma(\ell) = \int_0^\ell w'(x) dx - \int_0^\ell \beta(x) dx = w^2 - w^1 + \frac{\ell}{2}(\beta^1 + \beta^2). \quad (5)$$

For this particular element w_γ^1 is always zero. w_γ^2 is zero in the case of pure bending, which can be easily verified; take for instance the simple case where $w^1 = w^2$ and $\beta^1 = -\beta^2$. From these nodal values we compute a modified w_γ^* , simply by interpolation from the nodes,

$$w_\gamma^* = \frac{1}{2}(1-\xi)w_\gamma^1 + \frac{1}{2}(1+\xi)w_\gamma^2. \quad (6)$$

Eventually, the modified shear strains are obtained by differentiation of w_γ^* with respect to x (note that $d\xi/dx = 2/\ell$),

$$\gamma^* = \frac{dw_\gamma^*}{dx} = \frac{1}{\ell} (w^2 - w^1) + \frac{1}{2} (\beta^1 + \beta^2). \quad (7)$$

These shear strains are free from artificial constraints and the corresponding strain displacement matrix leads to a locking-free element. In fact, for the linear Timoshenko beam element, the resulting stiffness matrix is identical to the one obtained by reduced integration or an assumed strain method with $\xi = 0$ as sampling point. Certainly, these simple correlations are not directly transferable to the case of multidimensional elements.

Stabilized DSG Plate and Shell Elements

The extension of this method to shear deformable (“Reissner-Mindlin”) plates and shells is straightforward and described in detail in Bletzinger et al. [4] as well as Bischoff and Bletzinger [2]. The idea is to compute discrete shear gaps for transverse shear strains γ_ξ and γ_η , defined in the local element coordinate system, by integration of the corresponding kinematic equation in ξ - and η -direction, respectively. Interpolation and partial differentiation are carried out separately for $w_{\gamma\xi}$ and $w_{\gamma\eta}$. Thus, in contrast to the derivation for the beam element, there is no unique split of the total deformation, but one for each direction.

While avoiding formal details – which can be found in the aforementioned papers – there are some issues which are worth a comment. First of all, the four-node DSG element turns out to be exactly identical to the bilinear ANS element by Dvorkin and Bathe [7] (also known as the MITC-4). This similarity, however, is not directly transferable to triangles. In fact, triangular DSG elements do not seem to have exact correspondents in the existing literature.

As in the linear triangle DSG-3 the transverse shear strains are constant within the element, one-point quadrature suffices for exact integration. It has to be mentioned that, regardless of the number of integration points, the element appears to exhibit one non-physical zero energy mode. This mode, however, is non-communicable and thus it does not cause trouble in practical situations (i.e. meshes with more than one element). The linear, triangular DSG element thus represents a two-dimensional element with the lowest possible expense: Three nodes and one quadrature point (there is obviously no way going below this limit). On the other hand, its accuracy comes close to its bilinear counterpart and thus to the well-respected MITC-4.

In order to overcome the problem of oscillating transverse shear forces and to reduce sensitivity to mesh distortion for the MITC-4 element, Lyly et al. [10] proposed the application of stabilization methods (see also Codina [6]). Those methods have been transferred successfully to DSG elements by Bischoff and Bletzinger [2], [3]. Without increasing numerical expense this procedure significantly reduces distortion sensitivity of the elements and – especially in the case of triangles – appears to be helpful to obtain smooth solutions for transverse shear forces.

The numerical test illustrated in Figure 1 is especially well-suited to detect distortion sensitivity of plate elements. Here, a linear analysis of a fully clamped quadratic plate ($\ell_x = \ell_y = 4.0$) under uniform load $q = 1.0 \cdot 10^{-4}$ is carried out. Material data are $E = 30000$, $\nu = 0.3$. Using symmetry, one quarter of the plate is discretized by a

structured mesh of 4×4 four-node elements (diagonal intersection of the individual elements leads to a corresponding mesh with triangles). On the right hand side of Figure 1 it is indicated how mesh distortion is controlled with parameter d , which is varied from $d = 0$ to $d = 0.25$.

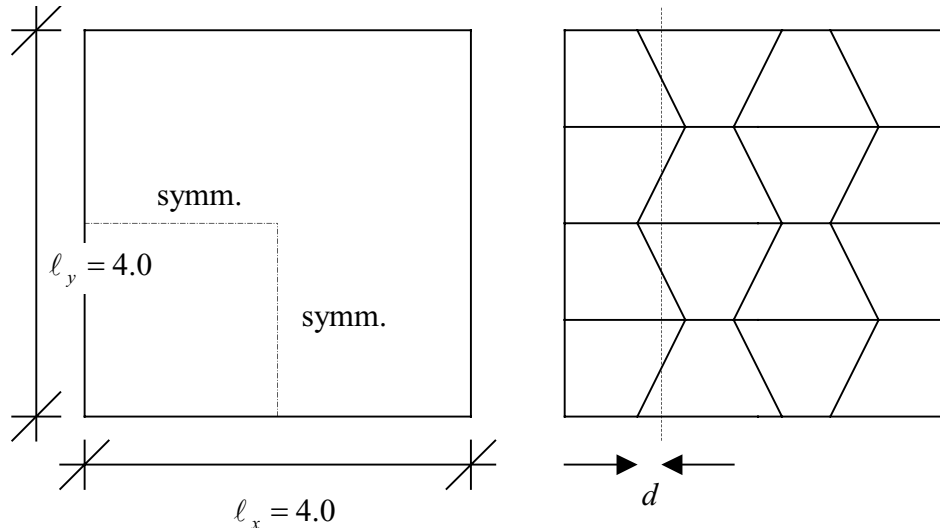


Figure 1 Sensitivity to mesh distortion, problem setup

In a first test, the distortion parameter d is fixed and the thickness of the plate is varied. A scaling of the load with t^3 ensures that, in the thin limit, the displacement is independent of the thickness (Kirchhoff-solution). The diagram in Figure 2 shows that without stabilization the elements are too stiff in the case of very thin plates.

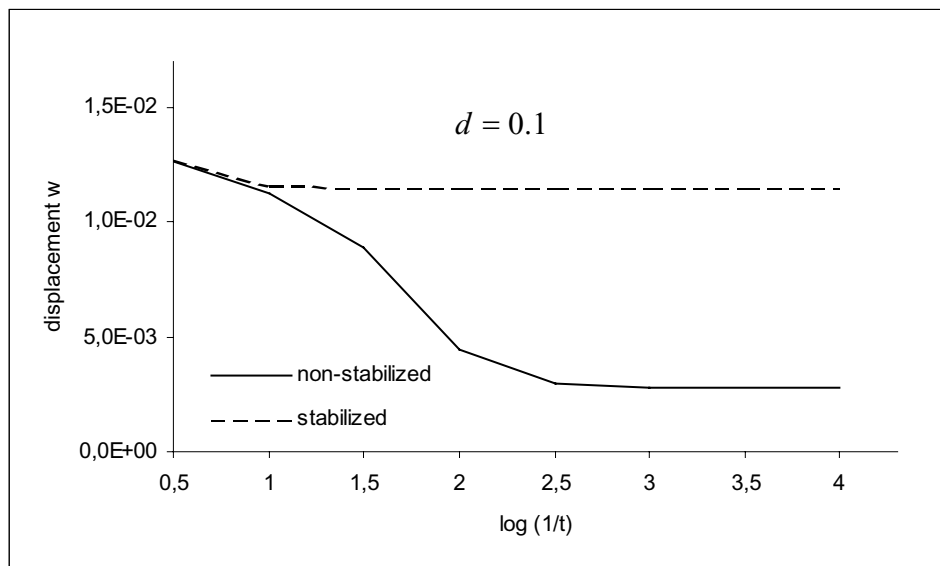


Figure 2 Distortion sensitivity, constant mesh – varying thickness

Figure 3 shows the results obtained for thickness $t = 0.01$ and varying distortion parameter. While the results of the stabilized element are almost constant with re-

spect to d , the non-stabilized version gets much too stiff as mesh distortion is increased. The results of both numerical tests are practically the same for triangular and quadrilateral elements. It should be mentioned once again that the distortion sensitivity of the non-stabilized elements is not a specific feature of the DSG formulation, but shared by other concepts, like the ANS method.

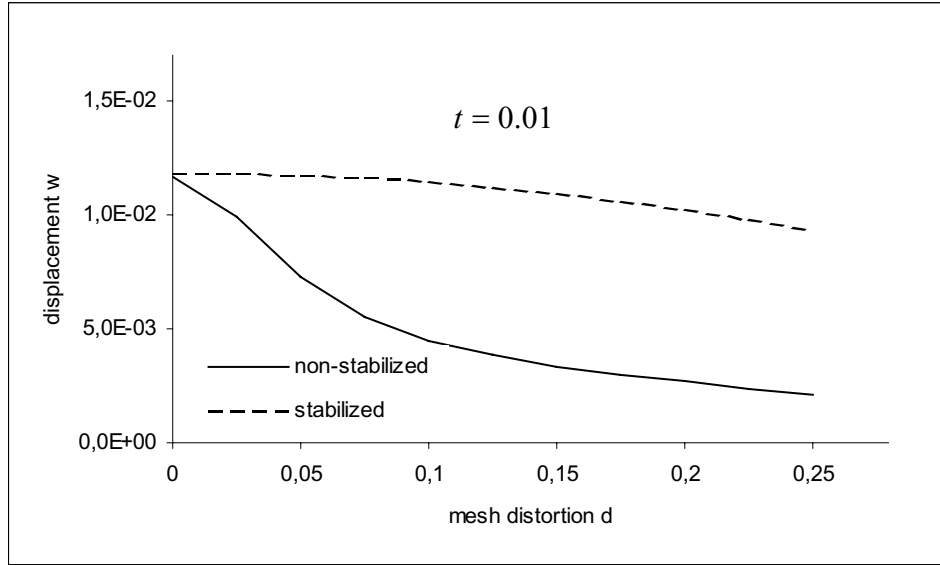


Figure 3 Distortion sensitivity, constant thickness – varying mesh distortion

Discrete Strain Gap Method

The main objective of this paper is to present the extension of the discrete shear gap method to general situations, rephrasing DSG as ‘discrete *strain gap*’ (see also Koschnick et al. [9]). In fact it is possible to tackle not only transverse shear locking in plate and shell elements, but – with the exception of volumetric locking – *all* locking effects appearing in structural finite elements. To this end we reinterpret the procedure described by equations (4) and (5) formally as the integration of a kinematic equation to discrete nodal strain gaps. This more general viewpoint can be applied to all kinds of structural finite elements.

Let us first consider the case of a two-dimensional plane stress element. The linearized strain components in curvilinear coordinates read

$$\varepsilon_{\xi\xi} = \mathbf{u}_{,\xi} \cdot \mathbf{g}_{\xi}, \quad \varepsilon_{\eta\eta} = \mathbf{u}_{,\eta} \cdot \mathbf{g}_{\eta}, \quad \varepsilon_{\xi\eta} = \frac{1}{2} (\mathbf{u}_{,\xi} \cdot \mathbf{g}_{\eta} + \mathbf{u}_{,\eta} \cdot \mathbf{g}_{\xi}). \quad (8)$$

with $\mathbf{g}_{\xi} = \mathbf{x}_{,\xi}$ and $\mathbf{g}_{\eta} = \mathbf{x}_{,\eta}$ representing the covariant base vectors of the corresponding coordinate system. In the context of a finite element formulation, the curvilinear coordinates ξ, η are identified with the natural element coordinate system.

While extending the DSG concept into multiple dimensions, the question arises, which kinematic equations, or which strain components, respectively, have to be integrated with respect to which coordinate direction. For reasons elaborated below we choose the following rule:

$$\begin{aligned}\mathcal{E}_{\xi\xi}^* &= \sum_{K=1}^N N_{,\xi}^K \int_{\xi_1}^{\xi_K} \mathbf{u}_{,\xi} \cdot \mathbf{g}_{\xi} d\xi, \quad \mathcal{E}_{\eta\eta}^* = \sum_{K=1}^N N_{,\eta}^K \int_{\eta_1}^{\eta_K} \mathbf{u}_{,\eta} \cdot \mathbf{g}_{\eta} d\eta, \\ \mathcal{E}_{\xi\eta}^* &= \frac{1}{2} \sum_{K=1}^N N_{,\xi}^K \int_{\xi_1}^{\xi_K} \left(\sum_{L=1}^N N_{,\eta}^L \int_{\eta_1}^{\eta_L} (\mathbf{u}_{,\eta} \cdot \mathbf{g}_{\xi} + \mathbf{u}_{,\xi} \cdot \mathbf{g}_{\eta}) d\eta \right) d\xi.\end{aligned}\quad (9)$$

with

$$\mathbf{u}_{,\xi} = \sum_{K=1}^N N_{,\xi}^K \mathbf{u}^K, \quad \mathbf{g}_{,\xi} = \sum_{K=1}^N N_{,\xi}^K \mathbf{x}^K, \quad \mathbf{u}_{,\eta} = \sum_{K=1}^N N_{,\eta}^K \mathbf{u}^K, \quad \mathbf{g}_{,\eta} = \sum_{K=1}^N N_{,\eta}^K \mathbf{x}^K. \quad (10)$$

Here, N^K are the standard shape functions, ξ_K, η_K are nodal coordinates in the parameter space, N is the number of nodes per element. This particular choice, especially for the mixed term $\mathcal{E}_{\xi\eta}$, is not the only possibility and future research might indicate that other versions are preferable. However, it fits into the framework of the original DSG method and contains the plate and shell elements developed so far as a special case.

All integrals involved are defined in the parameter space of the element and can be obtained analytically in advance, for instance using a computer algebra system, or numerically within the code. The coding effort for the element, if a standard displacement formulation is available, is limited to replacing the strain displacement operator by the definitions given in equations (9). These definitions apply to both triangular and quadrilateral elements and they are independent of the polynomial order. Moreover, extension to three dimensions is obviously straightforward.

In order to clarify the procedure and as a means to explain in some more detail the reason for the specific choice of the given definition, let us consider a four node quadrilateral element with rectangular geometry (side lengths ℓ_x and ℓ_y , x, y aligned to the natural coordinate directions ξ, η). With

$$\xi_{K,K=1..4} = \{-1, 1, 1, -1\}, \quad \eta_{K,K=1..4} = \{-1, -1, 1, 1\}, \quad (11)$$

$$N^K = \frac{1}{4} (1 - \xi_K \xi) (1 - \eta_K \eta), \quad (12)$$

$$\mathbf{u} = [u_x \quad u_y]^T, \quad \mathbf{g}_{\xi} = [\ell_x/2 \quad 0]^T, \quad \mathbf{g}_{\eta} = [0 \quad \ell_y/2]^T. \quad (13)$$

we obtain for the normal strain in ξ -direction

$$\begin{aligned}\mathcal{E}_{\xi\xi}^* &= N_{,\xi}^2 \int_{\xi_1}^{\xi_2} \mathbf{u}_{,\xi} \mathbf{g}_{\xi} d\xi + N_{,\xi}^3 \int_{\xi_1}^{\xi_3} \mathbf{u}_{,\xi} \mathbf{g}_{\xi} d\xi \\ &= \frac{1}{4} (1 - \eta) \int_{-1}^1 \left(N_{,\xi}^1 u_x^1 \frac{\ell_x}{2} + N_{,\xi}^2 u_x^2 \frac{\ell_x}{2} + N_{,\xi}^3 u_x^3 \frac{\ell_x}{2} + N_{,\xi}^4 u_x^4 \frac{\ell_x}{2} \right) d\xi \\ &\quad + \frac{1}{4} (1 + \eta) \int_{-1}^1 \left(N_{,\xi}^1 u_x^1 \frac{\ell_x}{2} + N_{,\xi}^2 u_x^2 \frac{\ell_x}{2} + N_{,\xi}^3 u_x^3 \frac{\ell_x}{2} + N_{,\xi}^4 u_x^4 \frac{\ell_x}{2} \right) d\xi \\ &= \frac{\ell_x}{8} \left[(1 - \eta) (u_x^2 - u_x^1) + (1 + \eta) (u_x^3 - u_x^4) \right]\end{aligned}\quad (14)$$

Note that the contributions from nodes 1 and 4 vanish because $\xi_1 = \xi_4$ and thus the corresponding integrals are identically zero.

Analogously,

$$\varepsilon_{\eta\eta}^* = \frac{\ell_y}{8} \left[(1 - \xi)(u_y^4 - u_y^1) + (1 + \xi)(u_y^3 - u_y^2) \right], \quad (15)$$

$$\varepsilon_{\xi\eta}^* = \frac{1}{2} \left(\frac{\ell_x}{8} [u_x^4 - u_x^1 + u_x^3 - u_x^2] + \frac{\ell_y}{8} [u_y^2 - u_y^1 + u_y^3 - u_y^4] \right). \quad (16)$$

For a formulation in Cartesian coordinates the standard transformation rules apply to obtain ε_{xx} , ε_{yy} and ε_{xy} .

In equations (14) - (16) we first observe that the components $\varepsilon_{\xi\xi}$ and $\varepsilon_{\eta\eta}$ are identical to those of a standard displacement formulation. This is due to the fact that the element under consideration has a rectangular shape. In general, also these terms will differ from the standard format (this is, for instance, important to avoid curvature thickness locking, as will be demonstrated later).

Moreover, one can see the reason for the seemingly arbitrary integration of $\varepsilon_{\xi\xi}$ in ξ -direction and $\varepsilon_{\eta\eta}$ in η -direction. With the procedure at hand it is ensured that $\varepsilon_{\xi\xi}$ varies linearly in η -direction and vice versa. These strain distributions are sensible for the in-plane bending modes (trapezoidal deformation of an individual element).

The third term $\varepsilon_{\xi\eta}$ – representing the in-plane shear strains in a rectangular element – is constant within the element. The analogy to reduced integration suggests the fact that the corresponding finite element will be free from shear locking. This will be discussed in more detail in the next section.

Bilinear 2D-Solid Element Q1-DSG

Using bilinear shape functions along with the formulae given in the previous section leads to the four-node 2d-solid element Q1-DSG which is investigated in the sequel. In order to check whether the element is free from shear locking, eigenvalue analyses of the stiffness matrix are performed. As a reference we take the well-established Q1-E4, based on the Enhanced Assumed Strain (EAS) method, proposed by Simo and Rifai [11] which is known to be free from shear locking. Comparison is also made to the standard displacement element Q1 which is not locking-free.

Figure 4 shows the results for the eigenvalue belonging to one of the in-plane bending modes which are crucial for shear locking. Q1-DSG produces exactly the same results as Q1-E4 and is thus confirmed to be locking-free. The eigenvalues of Q1 get higher (i.e. “stiffer”) as the aspect ratio of the element approaches infinity – the typical symptom for locking. Poisson’s ratio has been set to $\nu = 0$ in this example.

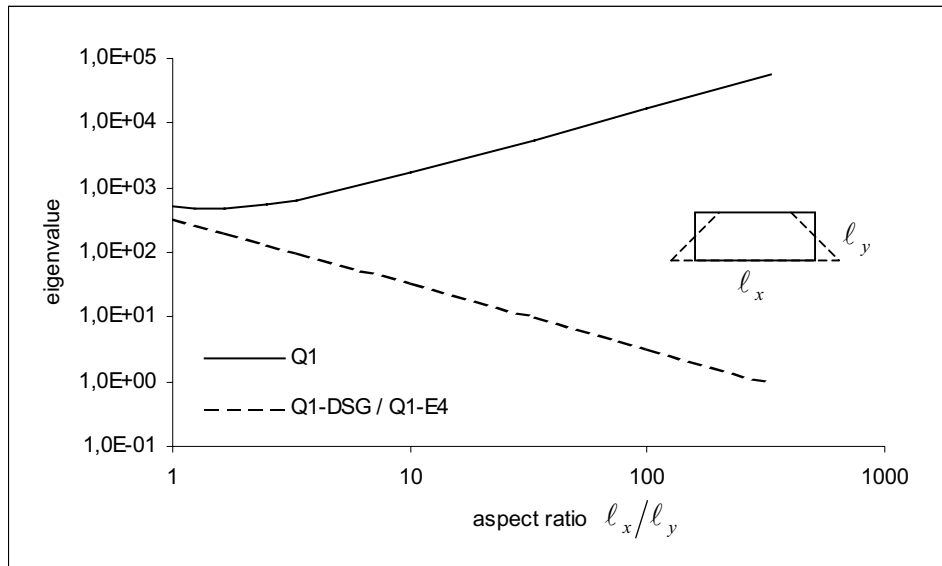


Figure 4 Eigenvalue analyses of element stiffness matrices, shear locking

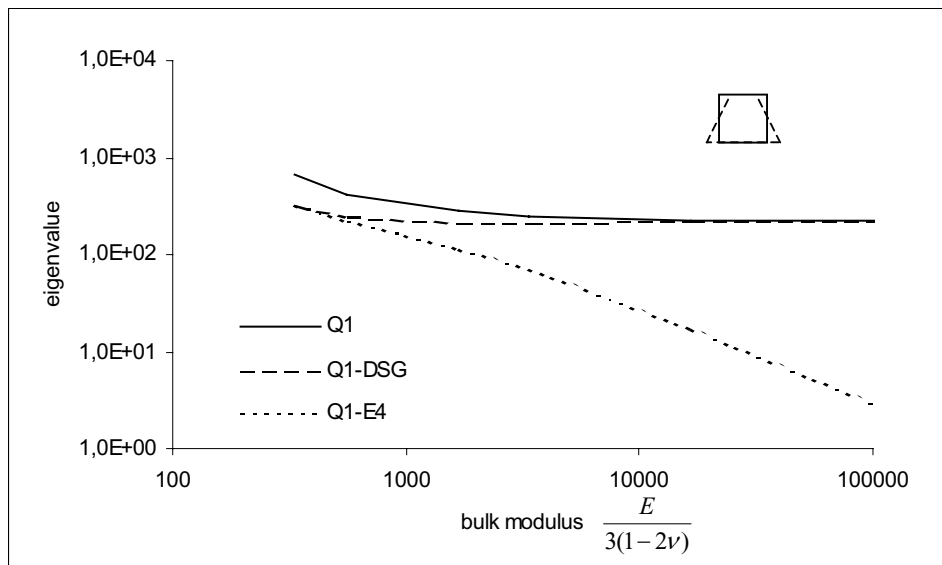


Figure 5 Eigenvalue analyses of element stiffness matrices, volumetric locking

If, for a fixed aspect ratio of 1, Poisson's ratio is gradually increased towards $\nu = 0.5$ the bulk modulus approaches infinity (the limit representing incompressible behavior) and volumetric locking comes into play. The results in Figure 5 demonstrate that in this case the situation is different. Both Q1 and Q1-DSG exhibit locking, while Q1-E4 is again locking-free. It has been mentioned already in the introduction that the DSG method only tackles "geometric" locking-effects but not volumetric locking which depends on material properties.

Another locking effect which is rarely discussed in the literature is called “curvature thickness locking” or sometimes “trapezoidal locking” (Sze [12]). It occurs in bending of initially curved structures when models are involved that include normal strains in thickness direction. This means that curvature thickness locking occurs in bending of curved beams or shells when the corresponding beam or shell elements include thickness strains (see for instance Büchter et al. [5]). Consequently it also shows up if 2d or 3d-solid elements are used to model curved, thin-walled structures (the name “trapezoidal locking” reflects the fact that in these cases the individual elements have a trapezoidal shape, cf. Figure 6).

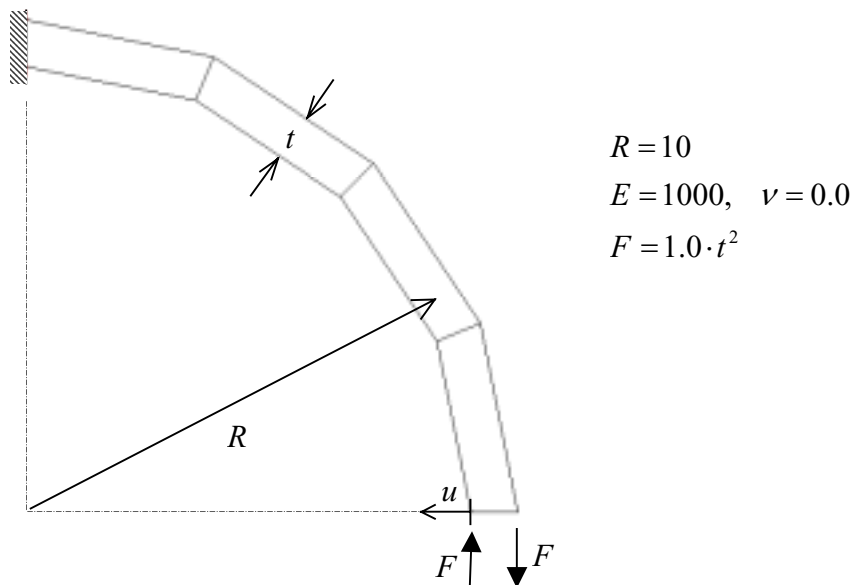


Figure 6 Bending of curved beam, problem setup

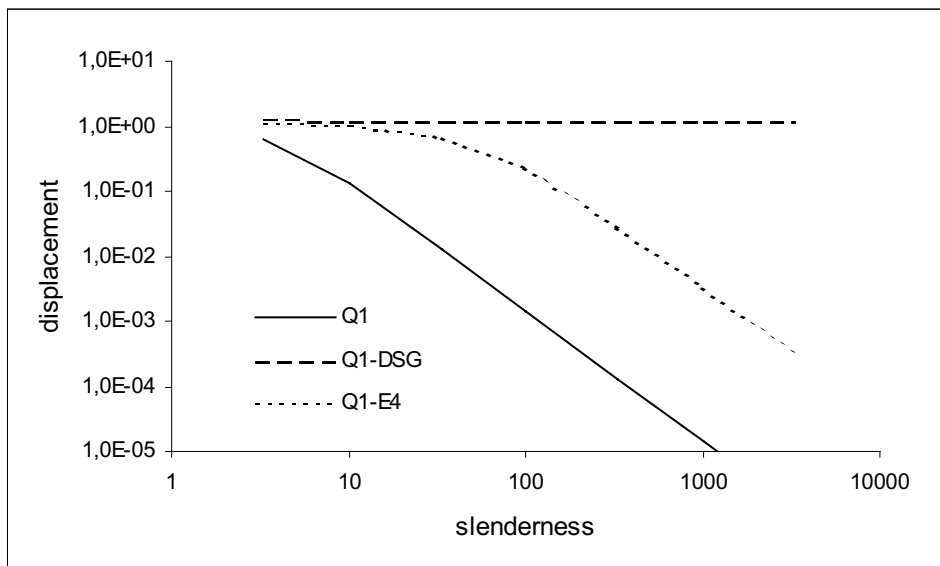


Figure 7 Bending of curved beam, curvature thickness locking (trapezoidal locking)

Figure 6 illustrates the problem setup for a numerical experiment to test the tendency of finite elements to exhibit curvature thickness locking. Note that the force F is scaled with the square of the thickness t^2 . Thus, the resulting moment $M = F \cdot t$ is proportional to t^3 , like the bending stiffness and consequently, the displacement u is independent of the thickness for the exact analytical solution.

In Figure 7 the results obtained with Q1, Q1-E4 and Q1-DSG are plotted versus the slenderness R/t of the beam. The present element turns out to be the only one which is locking-free. Both Q1 and Q1-E4 fail to represent the correct behavior. As already indicated, the reason is curvature thickness locking, resulting from parasitic transverse normal strains. The difference between Q1 and Q1-E4 results from shear locking which is not present in the EAS element.

This simple test problem may seem somewhat academic. However, it gains significance for instance in cases where shells are computed with 3d-solid elements. This can be the case if three-dimensional constitutive laws need to be applied, when transverse normal strain and stress effects become significant, or simply when no shell elements are available in a certain finite element code. The use of 3d-solid elements for the analysis of shells can also be sensible to facilitate transition between thin and thick parts of complex structures.

Biquadratic Shell Element Q2-DSG

Another application of the generalized DSG method presented in this paper is the problem of membrane locking in shells. As membrane locking only occurs in curved elements it is more pronounced when quadratic shape functions are used. Bilinear elements are free from locking when the elements are not warped, as for instance in the case of cylinders when structured meshes are used. Linear (triangular) elements are always free from membrane locking.

Membrane locking, like transverse shear locking and curvature thickness locking, results in an over-estimation of the bending stiffness and becomes more pronounced as the thickness approaches zero. A typical symptom are parasitic membrane stresses in the case of "inextensional bending" deformations.

In order to avoid membrane locking, we apply the general concept given by equations (9) to the membrane part of a biquadratic shell element (see also Koschnick et al. [9]). The corresponding formulation for the transverse shear strains $\varepsilon_{\xi\zeta}$ and $\varepsilon_{\eta\zeta}$ has already been presented earlier (see for instance Bischoff [1]) and follows the same pattern. For the numerical experiment presented in this section we will focus our attention on membrane locking.

In order to investigate whether the DSG method is capable of removing the effect of membrane locking in shell elements we return to the simple problem of a curved beam under bending. As we are now dealing with shell elements, this means that a small strip of a cylindrical shell is analyzed. Geometry, mesh and problem data are sketched in Figure 7.

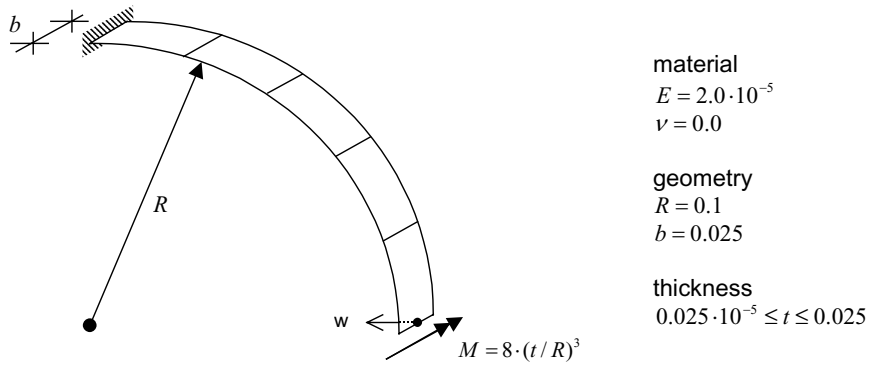


Figure 7 Bending of cylindrical shell, problem setup

Figure 8 summarizes the results obtained with Q2-DSG and the standard displacement element Q2. Again it can be recognized that application of the DSG method effectively removes locking. Note that transverse shear locking does not play a role for this special problem because already the standard displacement element Q2 is able to represent a constant bending moment without artificial transverse shear strains. Thus, the artificial stiffening effect observed in the diagram in Figure 8 is completely due to membrane locking.

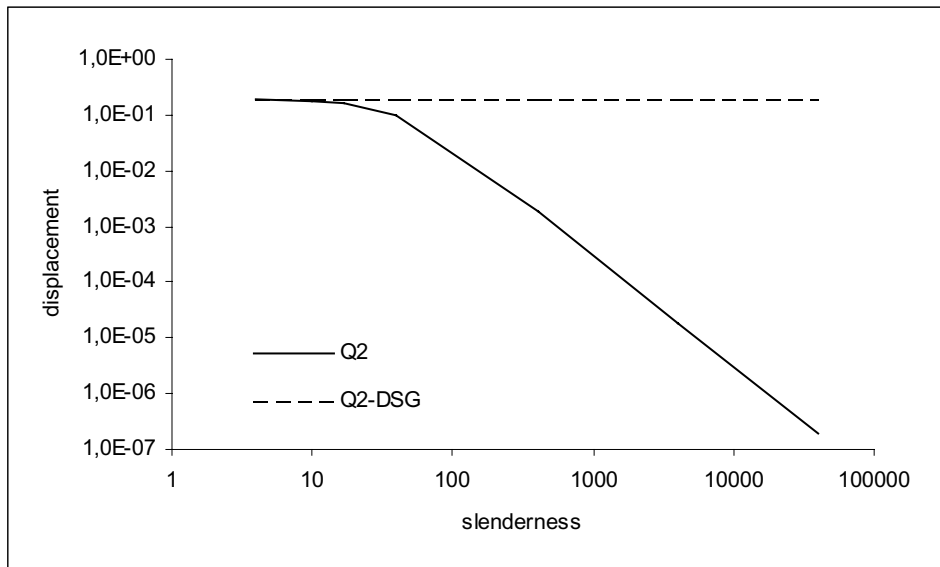


Figure 8 Bending of cylindrical shell, membrane locking

Convergence and the Patch Test

DSG elements do not satisfy the patch test for constant stresses if the elements are distorted within the “plane of integration” of the shear gaps. This means that Q1-DSG, as presented in one of the previous sections, is unable to represent a constant stress state if it is distorted in the $\xi\eta$ -plane (which is the only possible distortion anyway), because strains in ξ - and η -directions are modified. In contrast to that, DSG plate elements, where the transverse shear strains $\epsilon_{\xi\xi}$ and $\epsilon_{\eta\xi}$ are modified,

do satisfy the patch test, because also here the distortion occurs in the $\xi\eta$ -plane and no strains in this plane have been modified.

It is generally accepted that satisfaction of the patch test is mathematically neither necessary nor sufficient for convergence. We do not want to go into technical details of convergence of finite elements in this context. Under certain circumstances it can be stated that the significance of the patch test depends on the way the element stiffness matrix changes as the element size approaches zero: If there is some dependence on the element size, convergence can be achieved without satisfaction of the patch test. This is the case for plate and shell elements, where the side lengths go to zero while the thickness remains constant. Thus, in the limit of an infinite number of elements, the parts of the stiffness matrix which prevent satisfaction of the patch test vanish and convergence is guaranteed. The stiffness matrix of a 2d-solid element, however, does only depend on its *shape* but is independent of its *size* and thus there is no convergence if the patch test is not satisfied.

However, changes of the stiffness matrix in dependence of the element size can not only occur naturally, as in plates, but can also be introduced artificially, for instance with the help of stabilization methods (e.g. Hughes [8]). This is one possibility to ensure convergence for Q1-DSG in general cases. Efforts in this direction represent research in progress.

From a practical point of view, the situation appears to be less dramatic than it seems. First of all, convergence is in fact assured if, in the thin limit, element distortions vanish. This applies if structured meshes are used or if mesh refinement is achieved by element subsection. Moreover, the most important feature of an efficient finite element for practical applications is *coarse mesh* accuracy which is not directly connected to satisfaction of the patch test.

Summary and Conclusions

A generalization of the Discrete Shear Gap method to the Discrete *Strain* Gap method has been presented. The idea essentially involves integration of kinematic equations to discrete strain gaps at the nodes and subsequent interpolation and differentiation to obtain modified strain displacement relations. It has been shown that the method contains the potential to alleviate *all* geometric locking effects thus representing a unique methodology that could replace the numerous different concepts which are applied today to avoid different kinds of locking.

It is remarkable that, although the DSG method has originally been developed especially for transverse shear locking in plates and shells, no special adjustments or extensions of the basic concept were necessary to handle not only transverse shear locking, but also in-plane shear locking, curvature thickness locking and membrane locking.

Of course, the presented elements and the numerical experiments investigated in the present study only scratch the surface of a thorough development. Research efforts in the future will especially focus on convergence, either satisfying or circumventing the patch test and on distortion sensitivity. Moreover, it should be mentioned once again that volumetric locking cannot be cured with the DSG method and requires combination with other methods. It is, for instance, no problem to combine the DSG method and the EAS method within one element.

References

1. BISCHOFF, M. (1999) "Theorie und Numerik einer dreidimensionalen Schalenformulierungen", Ph.D. Thesis, Institut für Baustatik, Universität Stuttgart.
2. BISCHOFF, M., BLETZINGER, K.-U. (2001) "Stabilized DSG Plate and Shell Elements", Trends in Computational Structural Mechanics, CIMNE, Barcelona, pp. 253-263.
3. BISCHOFF, M. BLETZINGER, K.-U. "Improving stability and accuracy of plate finite elements via algebraic subgrid scale stabilization", submitted to: Computer Methods in Applied Mechanics and Engineering.
4. BLETZINGER, K.-U., BISCHOFF, M., RAMM, E. (2000) "A unified approach for shear-locking free triangular and rectangular shell finite elements", Computers and Structures 75, pp. 321-334.
5. BÜCHTER, N., RAMM, E., ROEHL, D. (1994) "Three-dimensional extension of nonlinear shell formulation based on the enhanced assumed strain concept", International Journal for Numerical Methods in Engineering 37, pp. 2551-2568.
6. CODINA, R. (2001) "Finite element approximation of the Reissner-Mindlin plate problem using subgrid scale stabilization", Trends in Computational Structural Mechanics, CIMNE, Barcelona, pp. 264-272.
7. DVORKIN, E.N., BATHE, K.-J. (1984) "A continuum based four-node shell element for general nonlinear analysis", Engineering Computations 1, pp. 77-88.
8. HUGHES, T.J.R. (1995), "Multiscale phenomena: Green's functions, the Dirichlet-to-Neumann formulation, subgrid scale models, bubbles and the origins of stabilized formulations", Computer Methods in Applied Mechanics and Engineering 127, pp. 387-401.
9. KOSCHNICK, F., BISCHOFF, M., BLETZINGER, K.-U. (2002) "Avoiding membrane locking with the DSG method", Proceedings of WCCM V, <http://wccm.tuwien.ac.at>.
10. LYLly, M., STENBERG, R., VIHINEN, T. (1993) "A stable bilinear element for the Reissner-Mindlin plate model", Computer Methods in Applied Mechanics and Engineering 110, pp. 343-357.
11. SIMO, J.C., RIFAI, S. (1990) "A class of mixed assumed strain methods and the method of incompatible modes", International Journal for Numerical Methods in Engineering 29, pp. 1595-1638.
12. SZE, K.Y. (2000) "On immunizing five-beta hybrid stress elements from 'trapezoidal locking' in practical analyses", International Journal for Numerical Methods in Engineering 47, pp. 907-920.